Chapter 4

Effect of Novel Corrosion Inhibitors on Electrical Properties of Cu Interconnect

4.1 Introduction

The CMP process for copper dual damascene has also been introduced as a new technology in IC manufacturing. This Cu CMP process employs a two step polishing process. The first step in Cu CMP is to remove the bulk of Cu, typically stopping on the underlying tantalum (Ta) diffusion barrier. Since Ta has quite different hardness as well as chemical properties compared to Cu, it is necessary to switch to different polishing slurry as a second step. The second step CMP process is carried out by the slurry that is used for removal of the diffusion barrier. During the CMP process, copper is oxidized to form cupric/cupreous oxides (CuO or Cu_2O) and copper hydroxides ($Cu(OH)_2$) passivation on copper surface [17]. As polishing with colloidal silica based slurry, it shows the strong absorption of colloidal silica on copper surface. This maybe related to that the colloidal silica chemisorbed onto the copper oxide layer by means of oxygen bonding [18]. It was difficult to remove colloidal silica by traditional post CMP cleaning. The residual polishing abrasives would contaminate the subsequent processing steps and cause lower yield in the finished integrated circuit.

The post-Cu CMP cleaning process involves buffing process with diluted nitric acid (HNO_3) and 1H-benzotriazole (1H-BTA, $C_6H_4N_3H$) aqueous solution, for colloidal silica removal and copper surface passivation. Cu(I)-BTA passivation on copper surface could surely prevent copper surface be corroded and reduce surface leakage current [21]. However, Cu(I)-BTA passivation would been decomposed above 150^{o}C. It would cause electrical property degradation. In this study, we would use HNO_3/DNNS or HNO_3/PBTC-Na_4 solution to form passivation on copper surface. The thermal stability and chemical durability of novel passivation layers would be investigated. Finally, we would study the effect of novel

passviation layers on electrical properties of copper interconnects and compared with Cu(I)-BTA passivation.

4.2 Experimental Procedures

4.2.1 Effect of Temperature on Passivation Layers

The substrates used in these experiments were 6-inch-diameter p-type (100) oriented silicon wafers. First, a 2000A thick SiO_2 was deposited by PECVD. After depositing, 500A thick Ta barrier metal layer and 1um thick Cu film was continuously deposited by sputtering. The Cu wafer was immersed in the HNO_3/DNNS ($0.1M/5E^{-2}M$) or HNO_3/PBTC-Na_4 ($0.6M/5E^{-3}M$) to form passivation layers on Cu surface for 3 minutes. Then, the Cu wafer was baked on the hot plate for 10 minutes. ESCA and contact angle analysis were performed to observe the effect of temperature on passivation layers.

Because blanket Cu film would reflect infrared ray used to rise temperature, it would result in error of real temperature. To carry out TDS analysis, the polished pattern Cu wafers were stacked Cu/Ta layer structure with a combination thickness of 1000/50 nm using shield mask. The pattern wafer was immersed in HNO_3/DNNS ($0.1M/5E^{-2}M$) and HNO_3/PBTC-Na_4 ($0.6M/5E^{-3}M$) to form passivation on Cu surface for 3 minutes. Following that, TDS analysis was performed.

4.2.2 Effect of Metal Chelators on Passivation Layers

The substrates used in these experiments were 6-inch-diameter p-type (100) oriented silicon wafers. First, a 2000A thick SiO_2 was deposited by PECVD. After depositing, 500A thick Ta barrier metal layer and 1um thick Cu film was continuously deposited by sputtering. The Cu wafer was immersed in the HNO_3 /DNNS ($0.1M/5E^{-2}M$) or HNO_3/PBTC-Na_4 ($0.6M/5E^{-3}M$) to form passivation layers on Cu surface for 3 minutes. Subsequently, the Cu wafer was immersed in metal chelators for 1 hour. Contact angle analysis was performed to

observe the effect of metal chelators on passivation layers.

4.2.3 Surface Morphology after Post-Cu CMP Cleaning

The substrates used in these experiments were 6-inch-diameter p-type (100) oriented silicon wafers. First, a 2000A thick SiO_2 was deposited by PECVD. After depositing, 500A thick Ta barrier metal layer and 1um thick Cu film was continuously deposited by sputtering. The polishing process was performed on a polisher (IPEC/Westech 372M) with colloidal silica based slurry on the embossed pad (RODEL Politex Regular^{TM}). The polishing recipes and slurry formulations were all listed in the Table.4-1. After polishing process, buffing with HNO_3/BTA or HNO_3/ DNNS or HNO_3/PBTC-Na_4 was used to remove colloidal silica and formation passivation layers. Following that, $5E^{-4}$M citric acid cleaning was performed on the SSEC-M50 cleaner during 40 cycles (15 cycles/min) and the Cu wafer was dry spun at the rotation rate of 2500 rpm. AFM analysis was used to determine the copper surface morphology after post-Cu CMP cleaning.

4.2.4 Effect of Passivation Layers on Surface Leakage Current

The Cu interconnect patterns were fabricated by the damascene process on 6-inch-diameter p-type (100) oriented silicon wafers. A 1.5um thick SiO_2 was deposited by PECVD, and the comb structure patterns for interconnects (Figure.4-1) were fabricated by conventional lithography and etching. The linewidth/space was 0.8um/0.8um. The depth of the trenches was 900nm. After depositing 50nm thick Ta barrier metal layer and 1.7um thick Cu film was continuously deposited by sputtering. The polishing process was performed to remove the excess metal. The polishing recipes and slurry formulations were listed in the Table.4-2. Table.4-3 listed the cleaning steps and parameters of SSEC-M50. Then, 500A SiN dielectric barrier was deposited by PECVD. The leakage current (I-V) was measured using HP4156C semiconductor parametric analyzer. Bias temperature stress (BTS) was performed

to enhance copper transport through ILD at 1.25MV/cm and 100^{o}C for 1four. After stress, the temperature was descended to room temperature. Following that, surface leakage current was measured.

AFM Analysis

In order to illustrate the ability of HNO_3/BTA, HNO_3/ DNNS, and HNO_3/ PBTC-Na_4 buffing to remove colloidal silica abrasives from the polished copper surface, the AFM (Digital Instruments DI 5000) was employed to scan the polished copper surface. The AFM operates by measuring the forces between a probe and the sample. There forces depend on the nature of the sample, the distance between the probe and the sample, the probe geometry, and sample surface contamination. The AFM principle is illustrated in Figure. 4-2. The instrument consists of a cantilever with a sharp tip mounted on its end. The cantilever is typically formed from silicon, silicon oxide, or silicon nitride. The cantilevers and tips are formed by depositing Si_3N_4 on a Si surface containing a pyramidal etch pit. The vertical sensitivity depends on the cantilever length. For topographic imaging, the tip is brought into continuous or intermittent contact with the sample and scanned across the sample surface. The motion of the cantilever is sensed by a segmented, position sensitive photodetector. Holding the signal constant, equivalent to constant cantilever deflection, by varying the sample height through a feedback arrangement, gives the sample height variation.

ESCA Analysis

ESCA (Americould Physical Electronics ESCA PHI 1600) was the high-energy version of the photoelectric effect. It was primarily used for identifying chemical species at the sample surface. When a solid is exposed to a flux of X-ray photons of known energy, photoelectrons are emitted from the solid. This photoelectron is emitted with a kinetic energy characteristic of the difference between the X-ray and the binding energy of the electron. The

energy of the emitted photoelectron defines the type of atom, and the number of photoelectrons at this energy is related to the number density of atoms present. Three basic components of ESCA (Figure.4-3) are the X-ray source, the spectrometer, and a high vacuum, even though such beam-induced chemistry as carbonization is minimized. The X-ray line width in ESCA should be as narrow as possible. Therefore, light element like Al ($E_{k\alpha}$=1.4866 keV) was common X-ray source. The ESCA electrons were detected by several types of detectors. The hemispherical sector analyzer consists of two concentric hemispheres with a voltage applied between them. A spectrum is generated by varying the voltage so that the trajectories of the electrons with different energies from the sample were brought to a focus at the analyzer exit slit. An electron multiplier amplifies the signal. In this study, electron spectroscopy for chemical analysis (ESCA) was employed to analysis the existence of passivation layers. Duo to DNNS has S atoms and PBTC-Na_4 has P atoms, we observed S atoms and P atoms to distinguish if DNNS and PBTC-Na_4 coordinate with Cu^+ ion on the Cu surface.

TDS Analysis

Thermal Desorption Spectroscopy (TDS, Hitachi Tokyo Electronics) was a mass analysis apparatus by heating the sample while contained in N_2 or Ar and simultaneously detecting the trace of out-gassing species transferred by carrier gas (N_2 or Ar) from the sample. As the temperature rises, not only absorbed or trapping species, but also the decomposed products of the substrate could be out-gassing species and they would be detected as a rise in ion intensity for a certain mass. This resulted in a specific-mass peak of the out-gassing species intensity versus temperature plot. The temperature at the maximum out-gassing mass peak would be related to the temperature activation energy for desorbing or decomposing reaction. Hence, the temperature stability of novel passivation layers could be evaluated by the mass detecting.

4.3 Results and Discussions

4.3.1 Thermal Stability of Passivation Layers

In order to sure that whether DNNS and PBTC-Na_4 could coordinate with Cu^+ ion on the Cu surface or not? ESCA was employed to analysis the existence of passivation layers. Because DNNS has S atoms, we observed S atoms to distinguish if DNNS coordinate with Cu^+ ion on the Cu surface. Figure.4-4 showed the ESCA spectra of copper film after immersed in HNO_3/DNNS solution. The S 2s and S 2p peaks were appeared. It indicated that DNNS could coordinate with Cu^+ ion on the Cu surface. Similarly, Figure.4-5 showed the ESCA spectra of copper film after immersed in HNO_3/PBTC-Na_4 solution. The P 2s and P 2p peaks were appeared. However, DNNS and PBTC-Na_4 passivation layers were very thin, so they usually could not be detected by ESCA analysis. Therefore, contact angle was performed to analysis the existence of hydrophobic passivation layers.

The results of contact angle analysis of temperature effect on passivation layers, as shown in Figure.4-6. The contact angle of BTA layer with temperature treatment of beyond 200^{o}C was close to the contact angle of pure Cu film about 30^{o}C. DNNS and PBTC-Na_4 passivation layers still were hydrophobic films at 200^{o}C. The temperature beyond 200^{o}C would destroy DNNS and PBTC-Na_4 passivation layers. The contact angle of passivation layers with temperature treatment of beyond 250^{o}C was close to the contact angle of pure Cu film. Figure.4-7 and Figure.4-8 showed the TDS spectra of copper film after immersed in HNO_3/DNNS and HNO_3/PBTC-Na_4 solution. They also indicated that DNNS and PBTC-Na_4 passivation would be decomposed above 200^{o}C.

4.3.2 Chemical Durability of Passivation Layers in Metal Chelators

The results of contact angle analysis after immersion of metal chelators were listed shown in Table.4-4. Three types of passivation layers almost were not damaged in the alkaline

environment of citric acid and acetic acid. Cu-BTA and DNNS passivation layers were hydrophobic films except after immersed in higher concentration and lower pH of citric acid. The result indicated that Cu-BTA and DNNS passivation layers were destroyed. Similarly, PBTC-Na_4 passivation layer was hydrophobic films except after immersed in higher concentration and lower pH of citric acid and acetic acid. Therefore, in order to prevent damaging DNNS and PBTC-Na_4 passivation layers during post CMP cleaning, we would use $5E^{-4}$M citric acid in latter experiment of evaluating passivation effect on surface leakage current.

4.3.3 Copper Surface Morphology

The AFM analysis of post-CMP cleaning with HNO_3/BTA buffing showed in Figure.4-9. As shown, a clean and planarization Cu surface was observed, which agreed with the result in the thesis of Kuo-Chin Hsueh [21]. Figure.4-10 to Figure.4-15 showed the AFM images of polished copper surface after post-CMP cleaning with various concentrations and time of HNO_3/DNNS buffing. It was found that the surface roughness increased as the buffing time increased. The best of surface planarity was reached at HNO_3/DNNS buffing ($0.1/1E^{-2}$M) for 1 min. Figure.4-16 to Figure.4-21 showed the AFM images of polished copper surface after post-CMP cleaning with various concentrations and time of HNO_3/ PBTC-Na_4 buffing. The buffing time and concentration of HNO_3/PBTC-Na_4 would dramatically influence the roughness of copper surface, too. Because buffing with HNO_3/DNNS ($0.1/1E^{-2}$M) for 1 min and HNO_3/PBTC-Na_4 ($0.6/1E^{-3}$M) for 3 min could obtain the cleanest surface and least roughness, the recipes would be chose in next experiment.

4.3.4 Result of Evaluating Passivation Effect on Surface Leakage Current

Result of passivation effect on surface leakage current, as shown in Figure.4-22. It showed that leakage current was similar before BTS and increased after BTS. This is due to

high temperature would damage passivation layers and cause Cu oxide formation. The proposed mechanism of dielectric degradation between Cu interconnects was shown in Figure.4-23 [42][43]. The general accepted dielectric degradation caused by copper includes the following steps [44][45]: (1) Cu ionization and injection of Cu^+ from the anode into the dielectric (2) drift of Cu^+ through the dielectric (3) completion of forming leakage passages and accumulation of Cu^+ near the cathode, which results in dielectric breakdown.

After Cu CMP process, the Cu surface was oxidized and Cu oxide was formed, and while SiH_4 gas flowed in SiN deposition, the Cu surface reacted to SiH_4 gas, and Cu-silicide was formed. In the surface layer of Cu oxide and Cu-silicide, some Cu atoms were ionized and easily move into the dielectric. Therefore, the key to improving dielectric characteristics was to eliminate Cu oxide formation and to prevent Cu-silicide reaction. In this study, passivation layers on copper surface could eliminate Cu oxide formation and prevent Cu-silicide reaction, so leakage current would be reduced [46]. Furthermore, due to DNNS passivation has the best thermal stability. It could obtain the lowest leakage current after BTS.

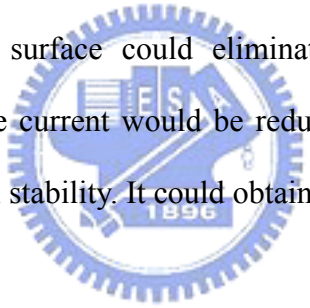

4.4 Summary

In this study, we studied the effect of passivation layers on electrical properties of Cu interconnects. First, thermal stability of passivation layers was discussed. According as results of contact angle measurement and TDS analysis, DNNS and PBTC-Na_4 passivation layers would be damaged beyond above 200^{o}C. Because DNNS passivation has the best thermal stability, it would prevent copper oxide formation and reduce Cu ionization. Hence, DNNS passivation could reduce surface leakage current after BTS.

In addition, chemical durability of passivation layers in metal chelators also was discussed. DNNS and PBTC-Na_4 passivation layers almost were not damaged in the alkaline environment of citric acid and acetic acid and were destroyed in higher concentration (0.2M) and lower pH (0.22) of citric acid. In order to prevent damaging passivation layers on Cu

surface during post CMP cleaning, we would use $5E^{-4}$M citric acid to remove Cu ions. Due to $5E^{-4}$M citric acid in the acidic environment has enough ability to remove the most Cu ions, describing in chapter 3.4.4.

,

Table.4-1 Polishing parameters for surface morphology evaluation.

IPEC 372M	***1st step***	***2nd step***	
Process	***Polishing***	***HNO_3/BTA buffing***	***HNO_3/DNNS or HNO_3/PBTC-Na_4 buffing***
Down force	5.0 psi	2.0 psi	2.0 psi
Back pressure	1.5psi	0 psi	0 psi
Platen/carrier speed	42/45 rpm	20/25 rpm	20/25 rpm
Slurry flow rate	150 ml/min		
Polishing Pad	Rodel Politex Regular E.™		
Carrier Film	Rodel R200 T3		
Slurry formulation	10% 100S + 10% H_2O_2	HNO_3/BTA ($0.6/1E^{-3}$M)	HNO_3/DNNS or HNO_3/ PBTC-Na_4
Polish time	1min	1min	parameter

Table.4-2 Polishing parameters of evaluating passivation effect on surface leakage current.

IPEC 372M	***Phase1*** ***Cu removing***	***Phase2*** ***Ta removing***	***Phase3*** ***Buffing***
Down force	5.0 psi	5.0 psi	2.0 psi
Back pressure	1.5 psi	1.5 psi	0 psi
Platen/carrier speed	42/45 rpm	42/45 rpm	20/25 rpm
Slurry flow rate	150 ml/min	150 ml/min	150 ml/min
Polishing Time	160 sec	180 sec	parameter
Polishing Pad	Rodel IC 1400™	Rodel Politex Regular E.™	
Carrier Film	Rodel R200 T3		
Slurry formulation	10% 100S + 10% H_2O_2	10% 50ck + 10% H_2O_2	HNO_3/BTA ($0.6/1E^{-4}$M) or HNO_3/DNNS ($0.1/1E^{-2}$M) or HNO_3/PBTC-Na_4 ($0.6/1E^{-3}$M)

Table.4-3 The cleaning steps and parameters of SSEC-M50

SSEC-M50		***Cleaning time***	***Flow rate***	***Rotation rate of water***
Step1	***Citric acid cleaning***	40 cycles (15 cycles/min)	150 ml/min	800 rpm
Step2	***DIW rinse***	7 cycles (15 cycles/min)	unknown	800 rpm
Step3	***Dry spin***	25 sec	off	2500 rpm

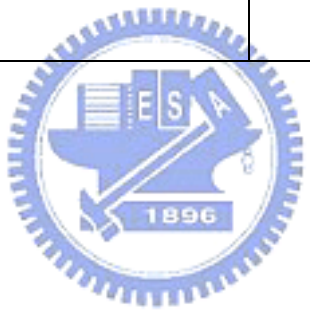

Table.4-4 The contact angle of passivation layers after immersion of metal chelators

Condition	***The result of contact angle***		
	HNO_3/BTA	***HNO_3/DNNS***	***HNO_3/PBTC-Na_4***
0.2M Citric acid with pH=0.22	31.5°	31.2°	33.7°
0.2M Citric acid with pH=9.32	71.8°	74.8°	77.3°
$5E^{-4}$M Citric acid with pH=1.98	73.4°	87.7°	82.4°
$5E^{-4}$M Citric acid with pH=9.22	81.3°	84°	82.6°
0.2M Acetic acid with pH=0.87	66.4°	63.1°	32.6°
0.2M Acetic acid with pH=9.27	76.3°	73.6°	72.2°
$5E^{-4}$M Acetic acid with pH=2.47	83.8°	86.5°	81.9°
$5E^{-4}$M Acetic acid with pH=9.25	81.9°	85.3°	85.1°

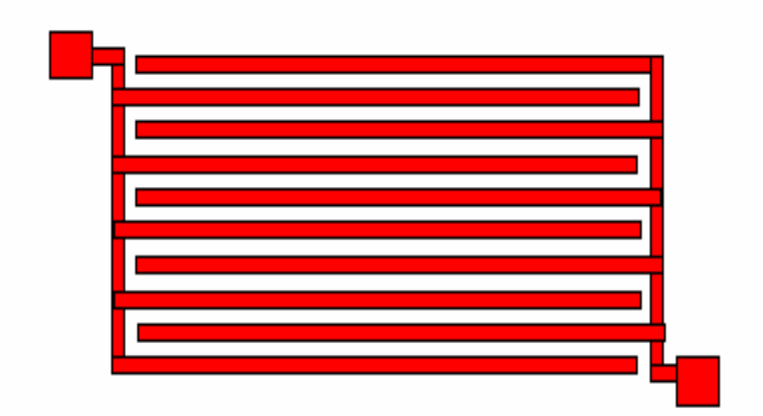

(a)

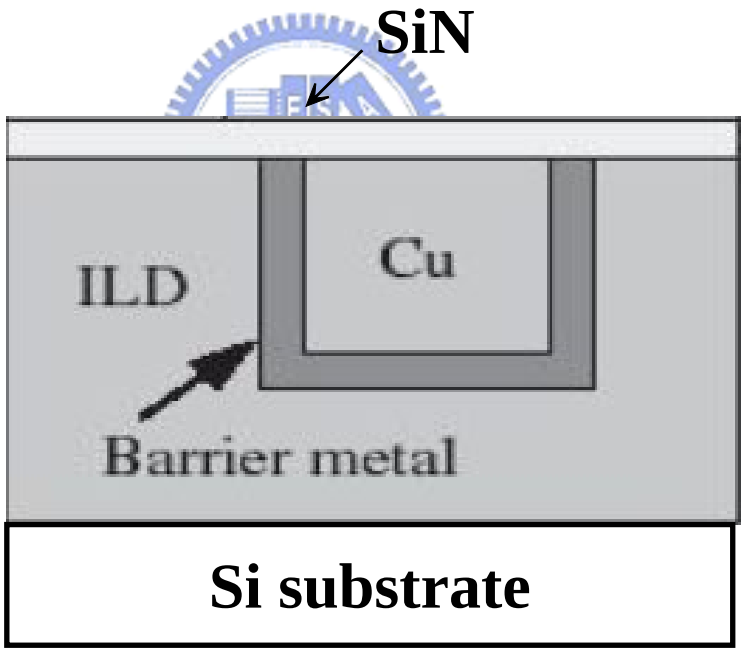

(b)

Figure.4-1 (a) Comb structure interconnect
(b) Cross-section of comb structure interconnect

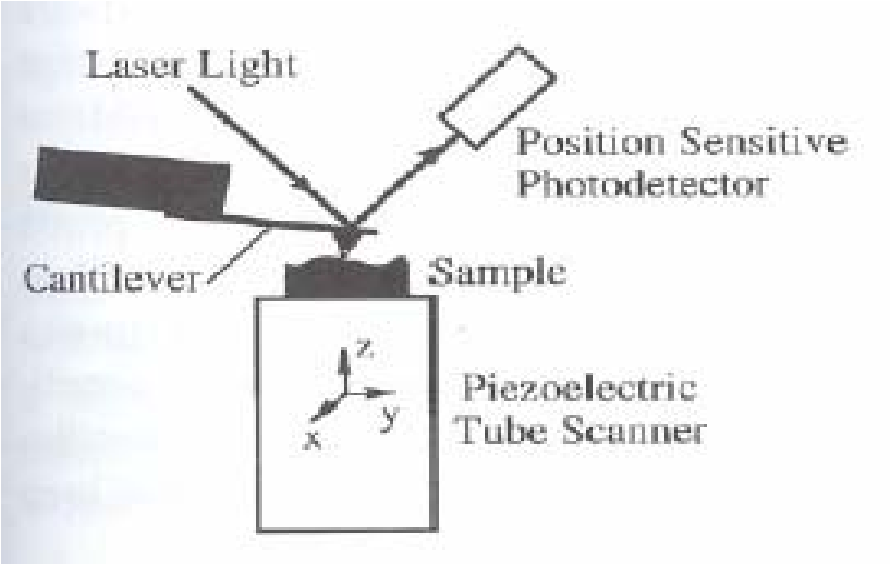

Figure.4-2 Schematic illustration of an AFM

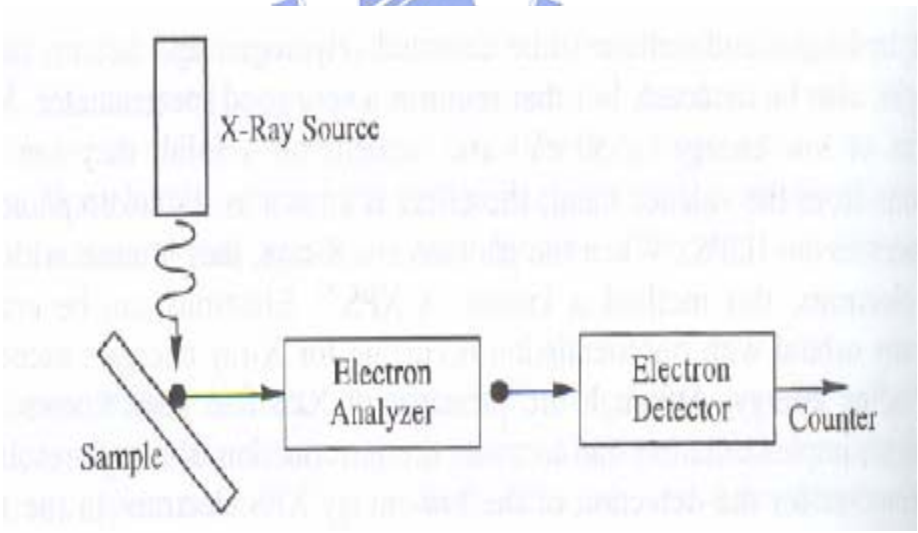

Figure.4-3 ESCA measurement schematic

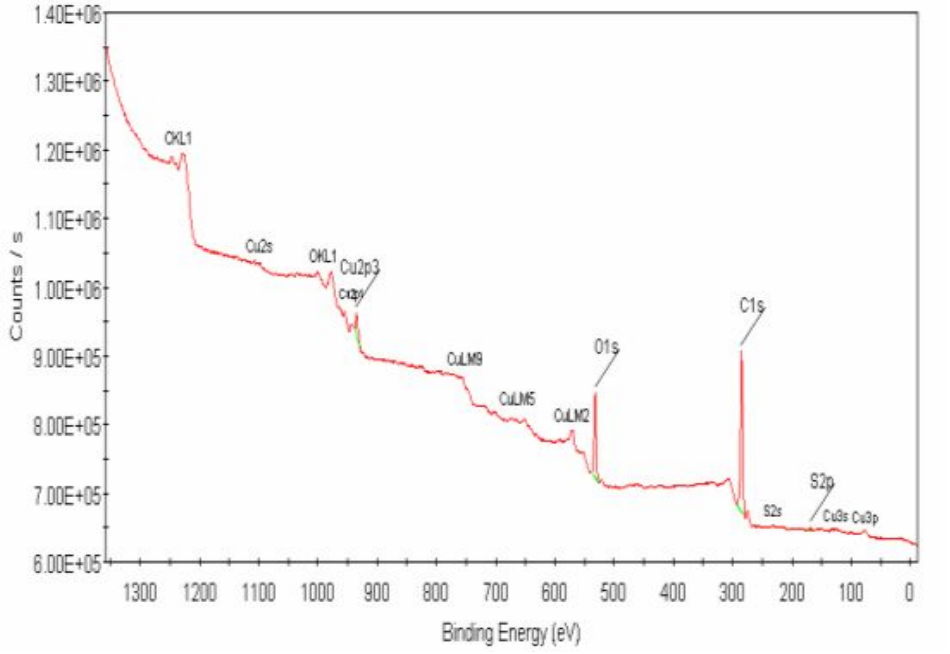

Figure.4-4 ESCA spectra of copper film after immersed in HNO_3/DNNS

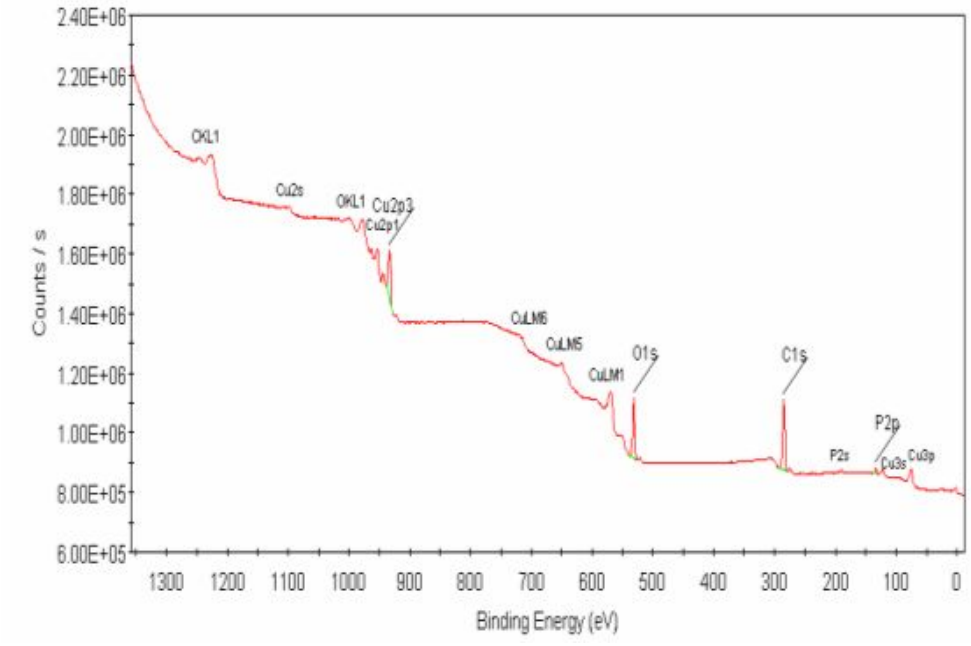

Figure.4-5 ESCA spectra of copper film after immersed in HNO_3/PBTC-Na_4

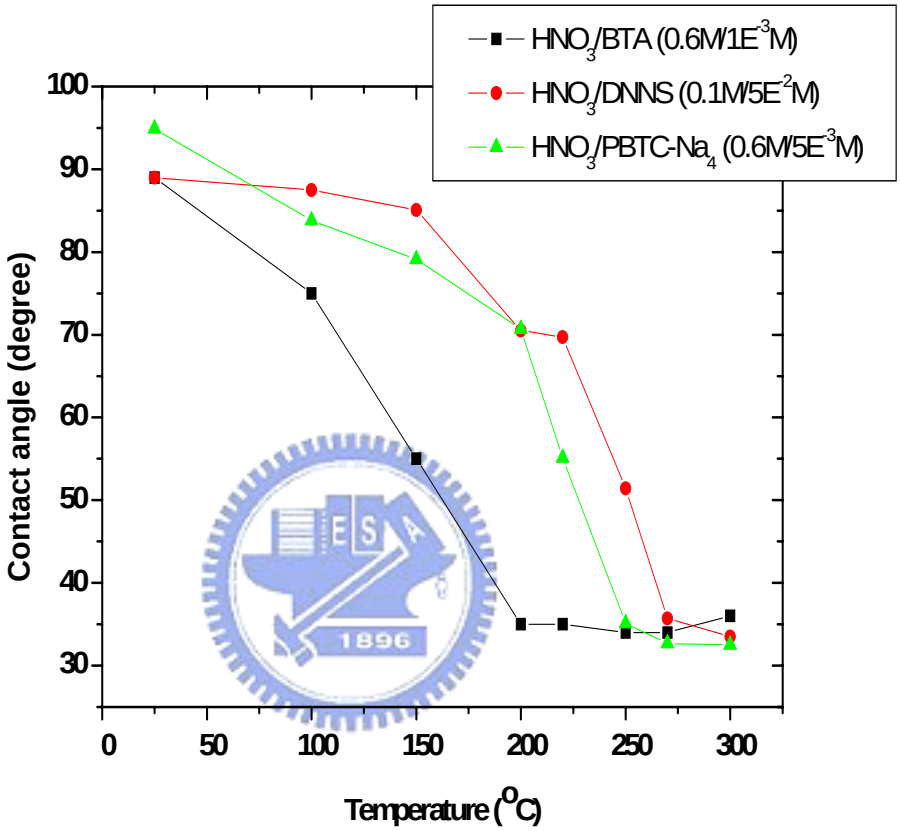

Figure.4-6 Contact angle analysis of temperature effect on passivation layers

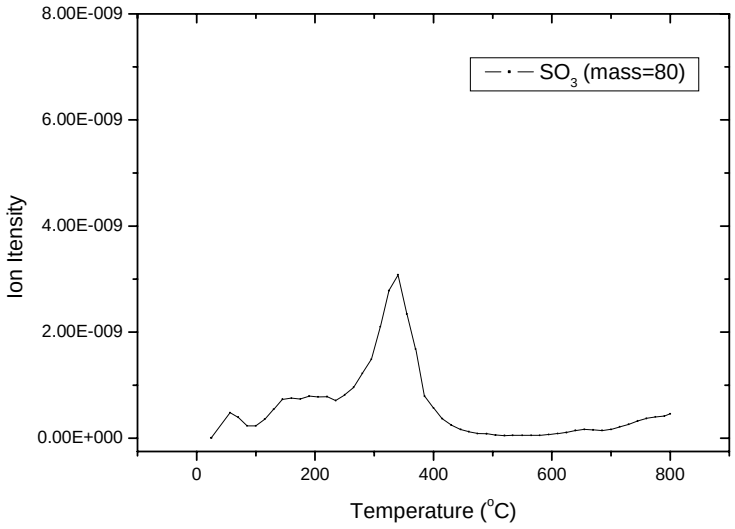

Figure.4-7 TDS spectra of pattern copper wafer after immersed in HNO_3/DNNS

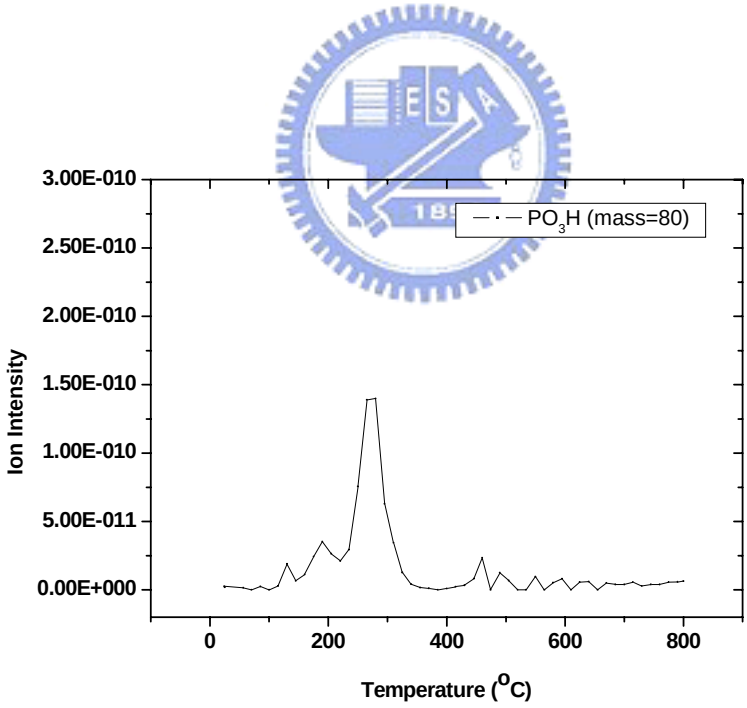

Figure.4-8 TDS spectra of pattern copper wafer after immersed in HNO_3/PBTC-Na_4

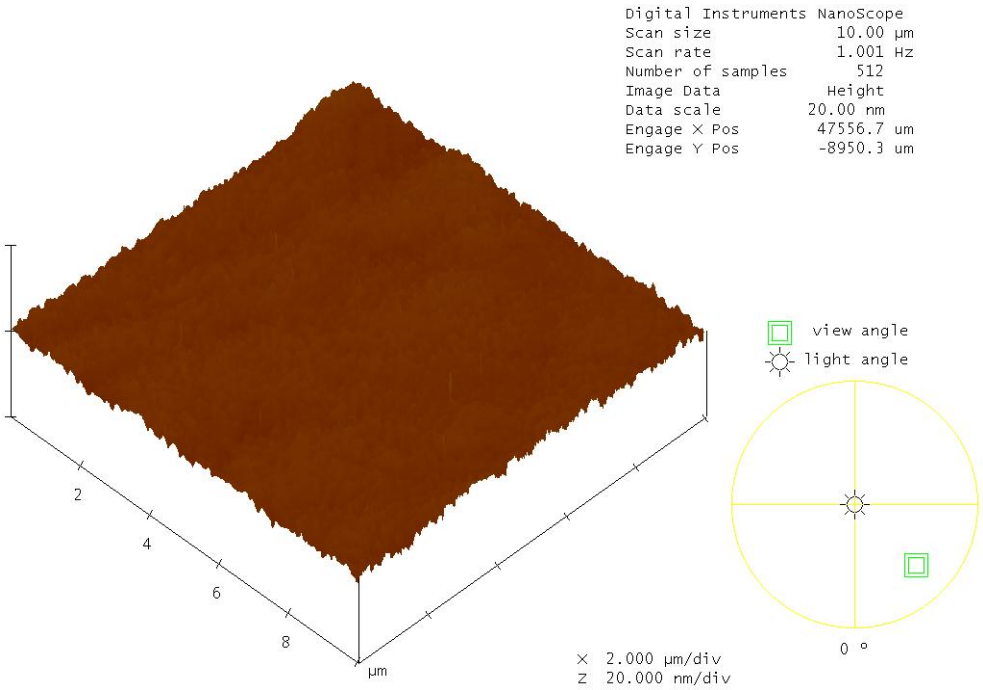

(a)

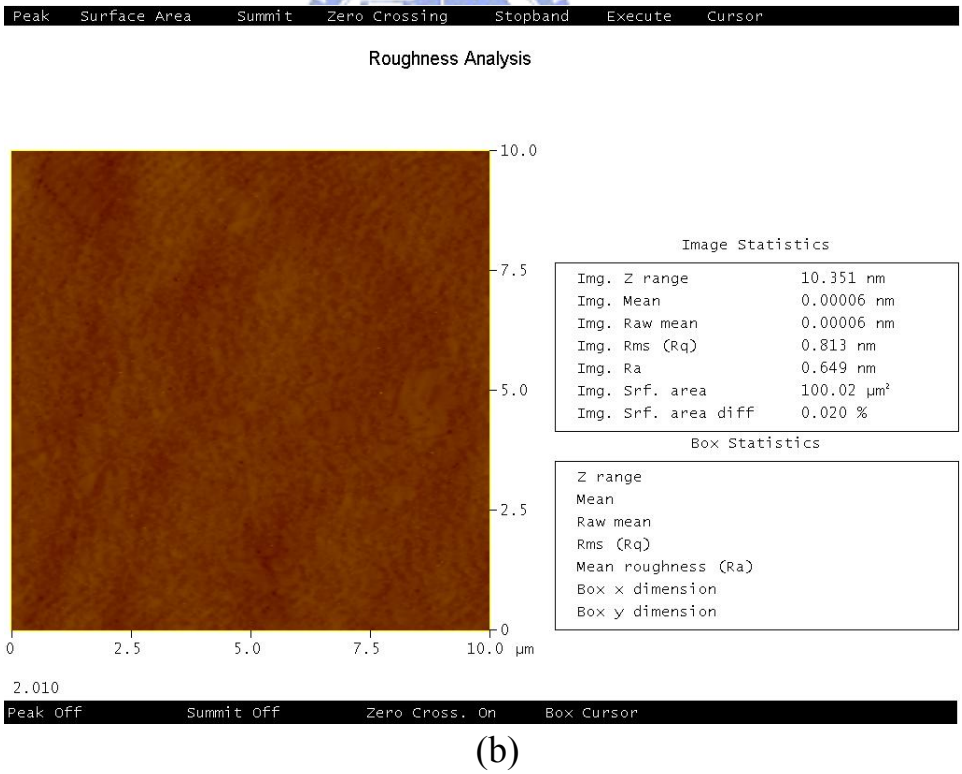

(b)

Figure.4-9 AFM images of polished copper film with HNO_3/BTA =0.6/1E^{-4}M buffing, buffing time=1min (a) 3D diagram (b)roughness analysis.

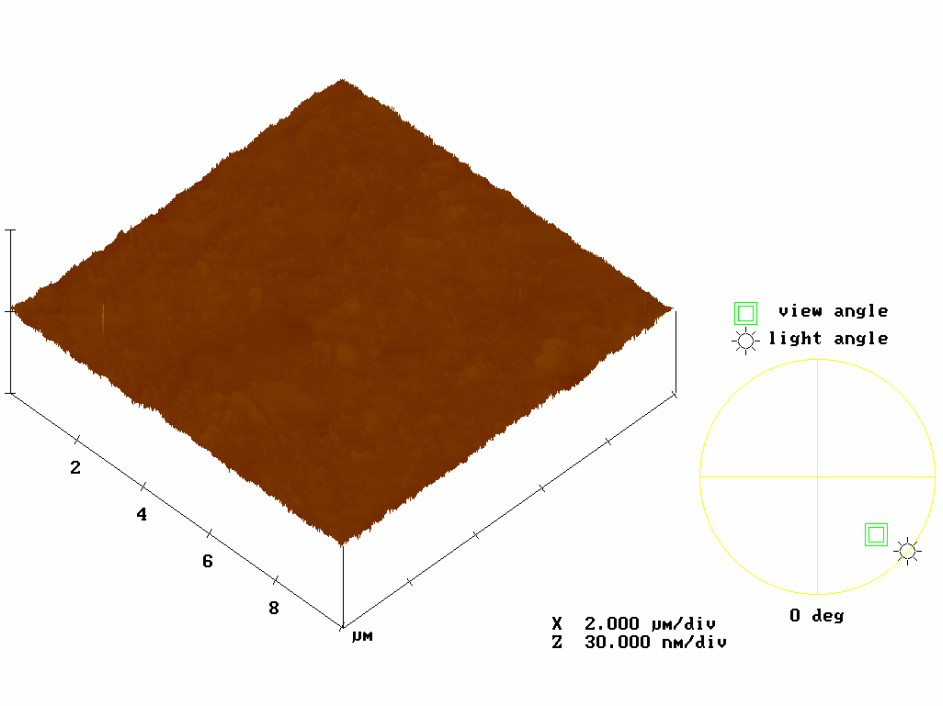

(a)

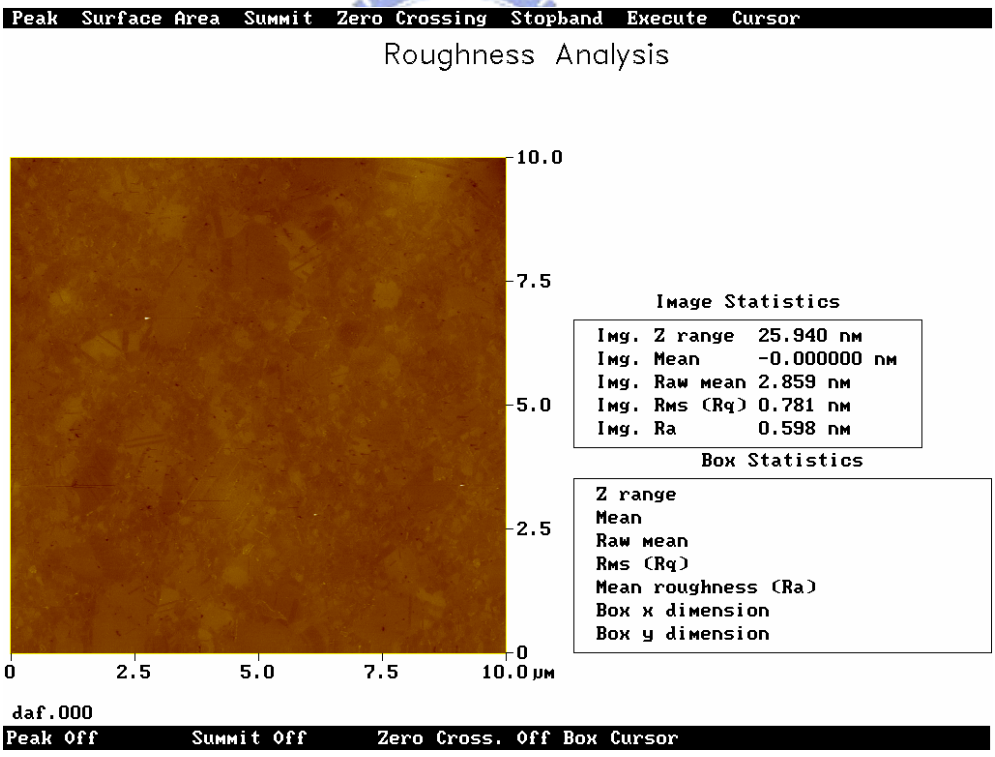

(b)

Figure.4-10 AFM images of polished copper film with HNO_3/DNNS =0.1/5E^{-2}M buffing, buffing time=1 min (a) 3D diagram (b)roughness analysis.

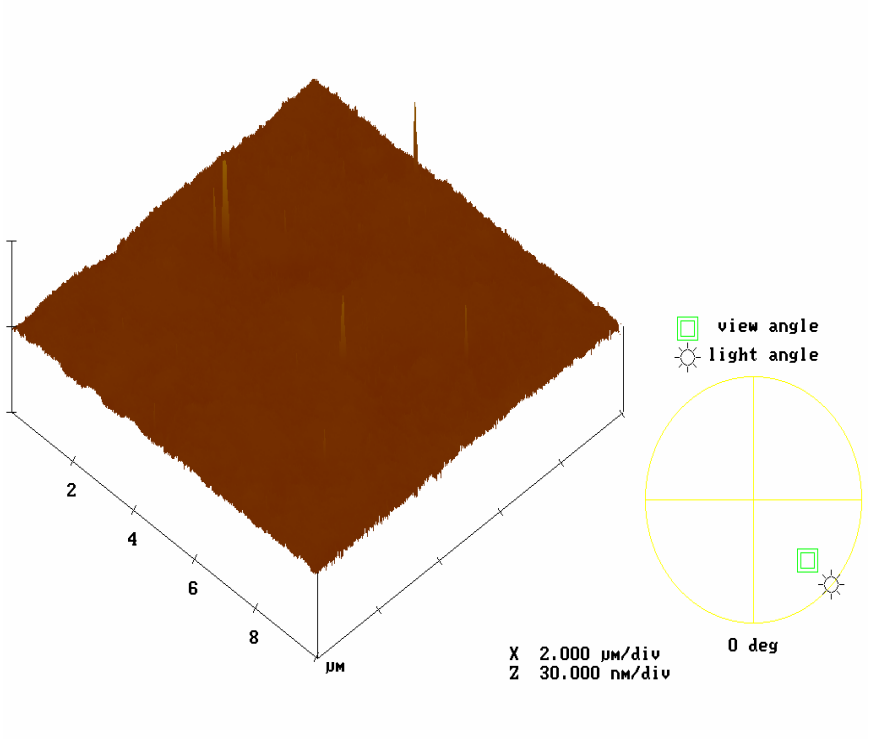

(a)

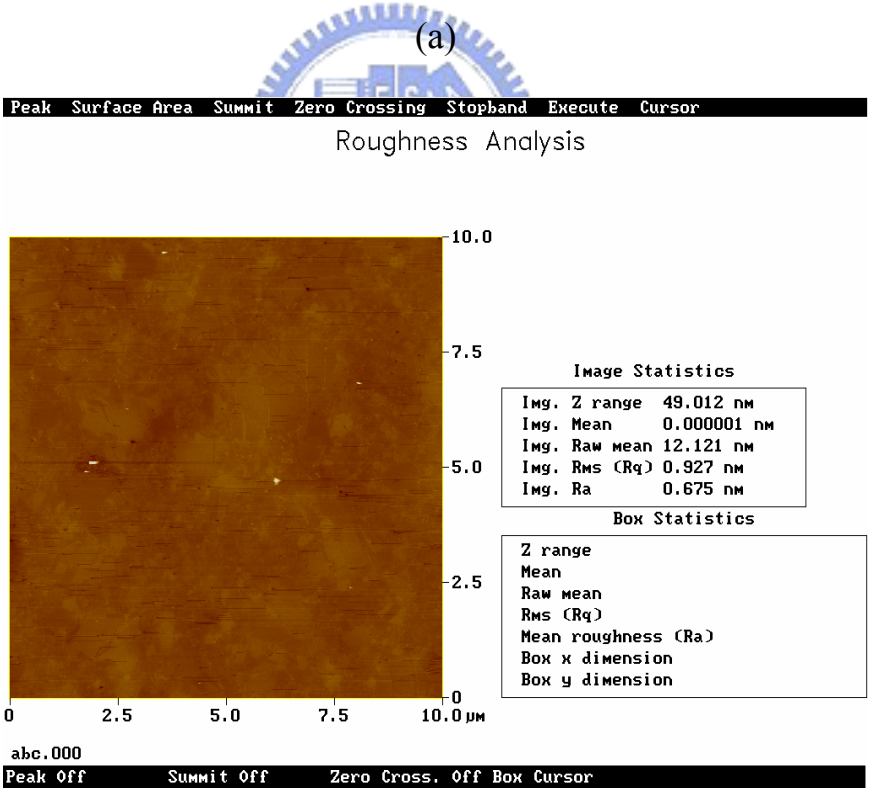

(b)

Figure.4-11 AFM images of polished copper film with HNO_3/DNNS =0.1/5E^{-2}M buffing, buffing time=3 min (a) 3D diagram (b)roughness analysis.

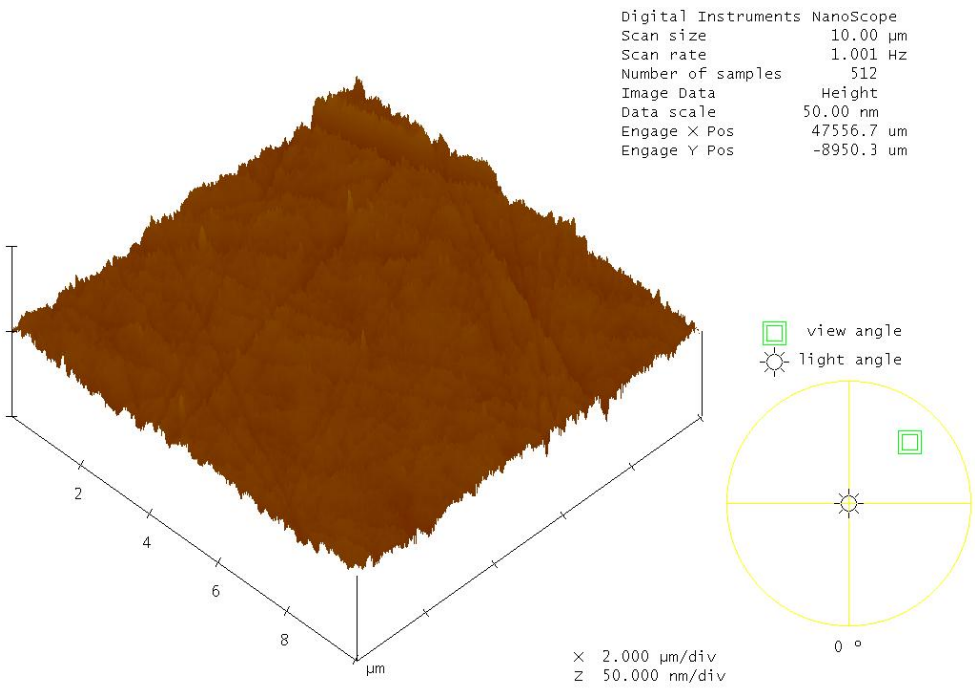

(a)

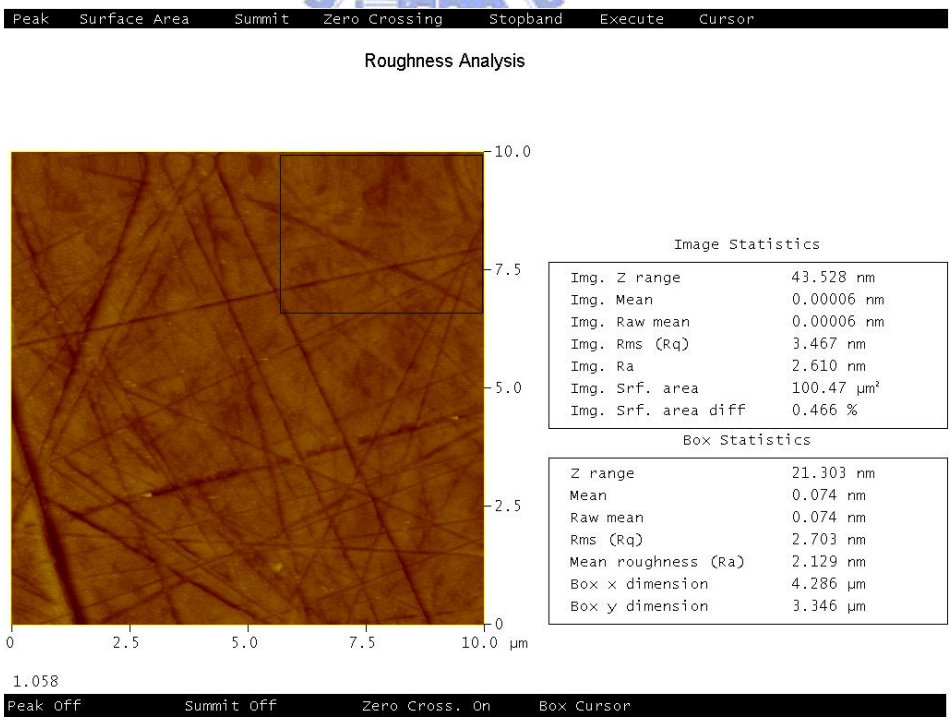

(b)

Figure.4-12 AFM images of polished copper film with HNO_3/DNNS =0.1/5E^{-2}M buffing, buffing time=6 min (a) 3D diagram (b)roughness analysis.

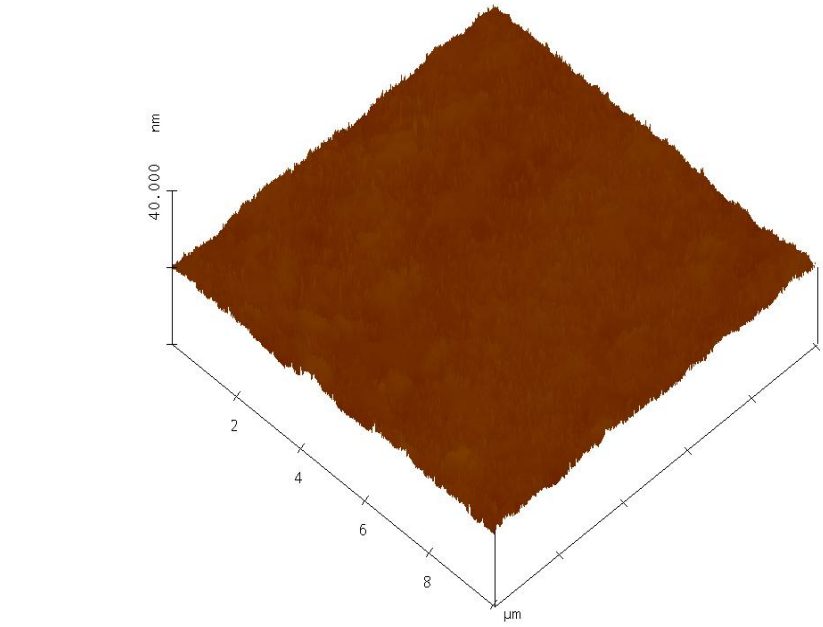

(a)

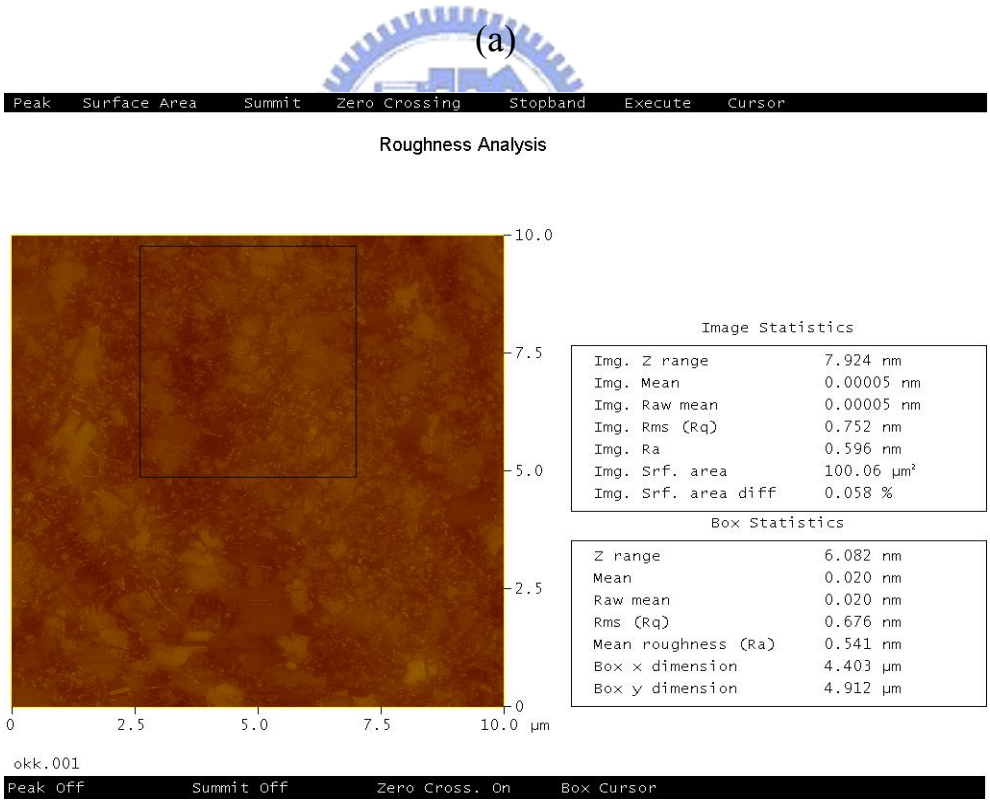

(b)

Figure.4-13 AFM images of polished copper film with HNO_3/DNNS =0.1/1E^{-2}M buffing, buffing time=1 min (a) 3D diagram (b)roughness analysis.

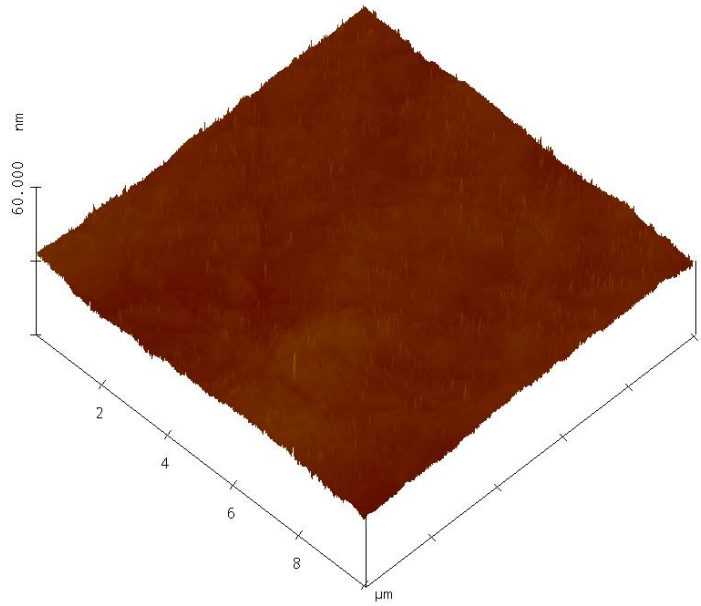

(a)

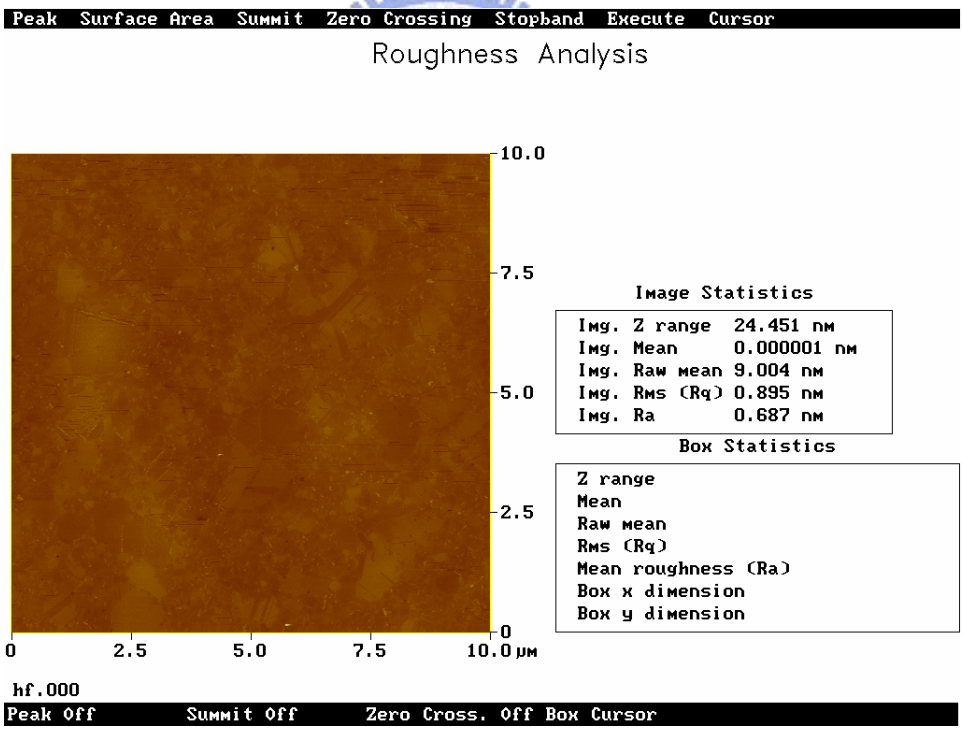

(b)

Figure.4-14 AFM images of polished copper film with HNO_3/DNNS =0.1/1E^{-2}M buffing, buffing time=3 min (a) 3D diagram (b)roughness analysis.

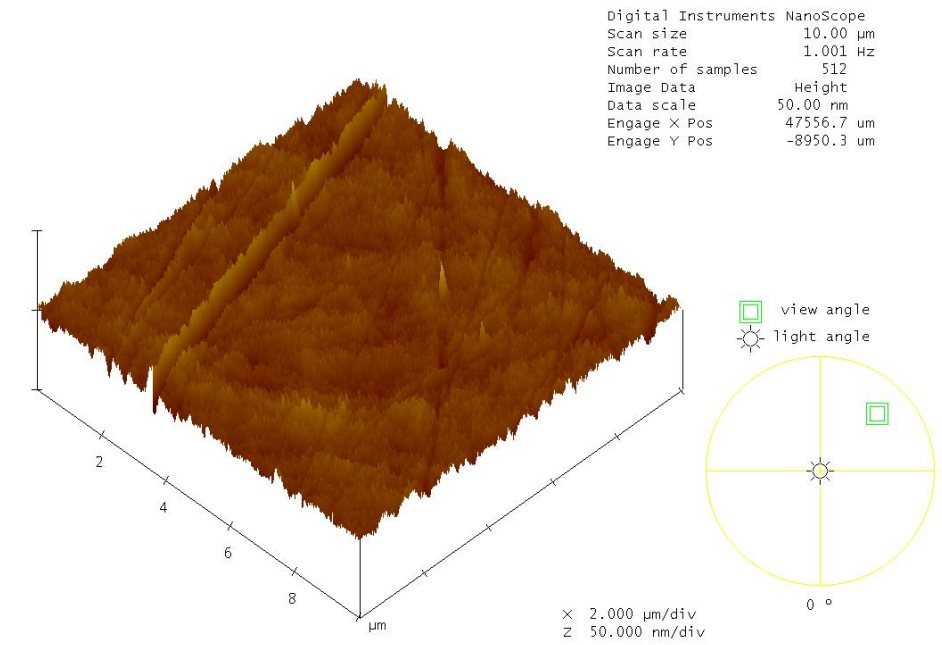

(a)

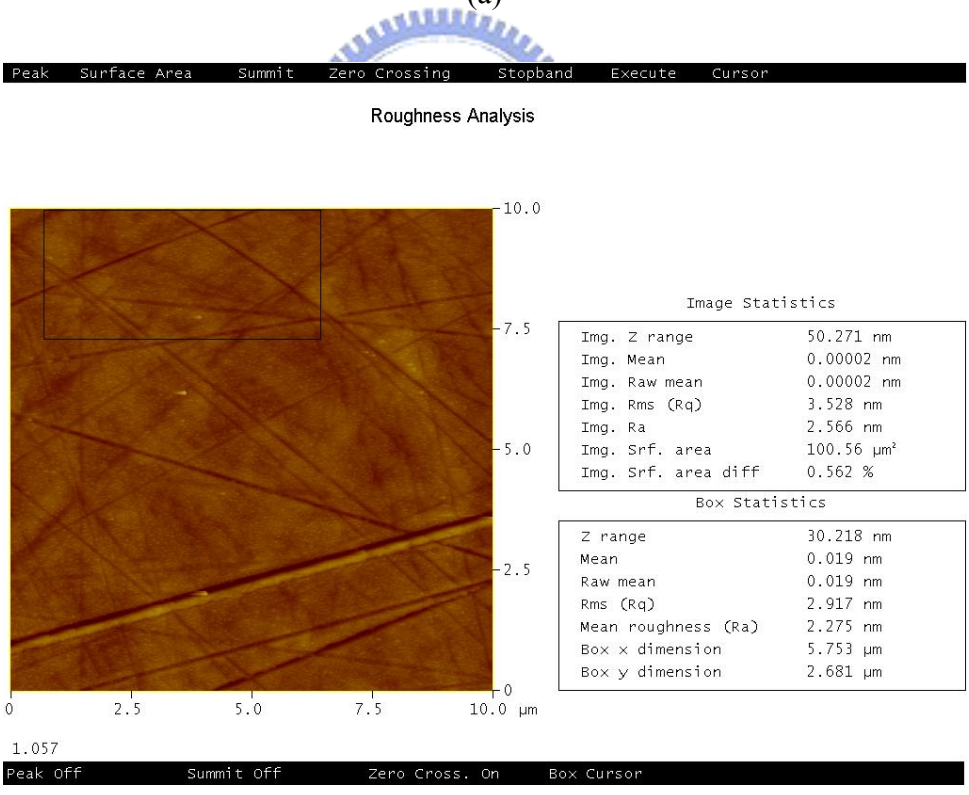

(b)

Figure.4-15 AFM images of polished copper film with HNO_3/DNNS =0.1/1E^{-2}M buffing, buffing time=6 min (a) 3D diagram (b)roughness analysis.

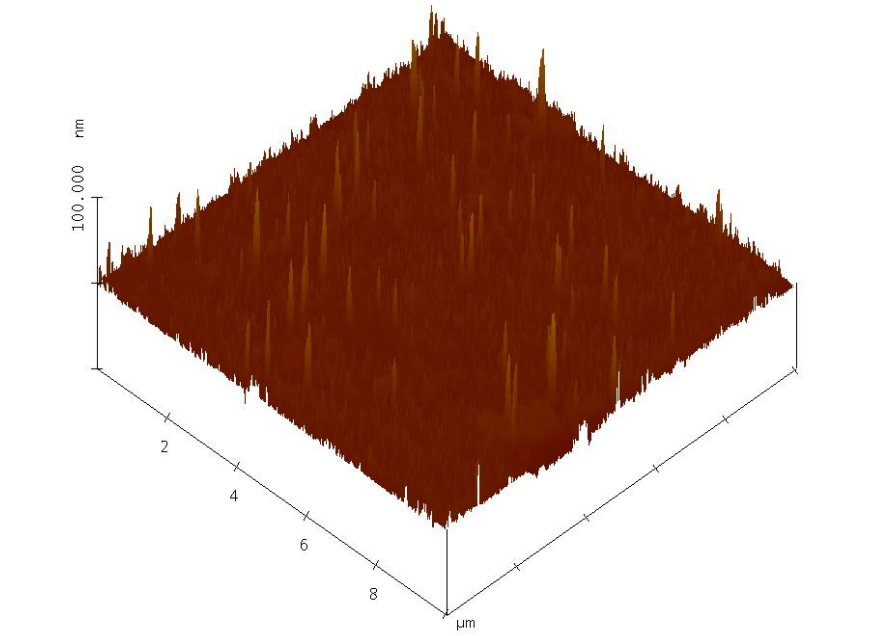

(a)

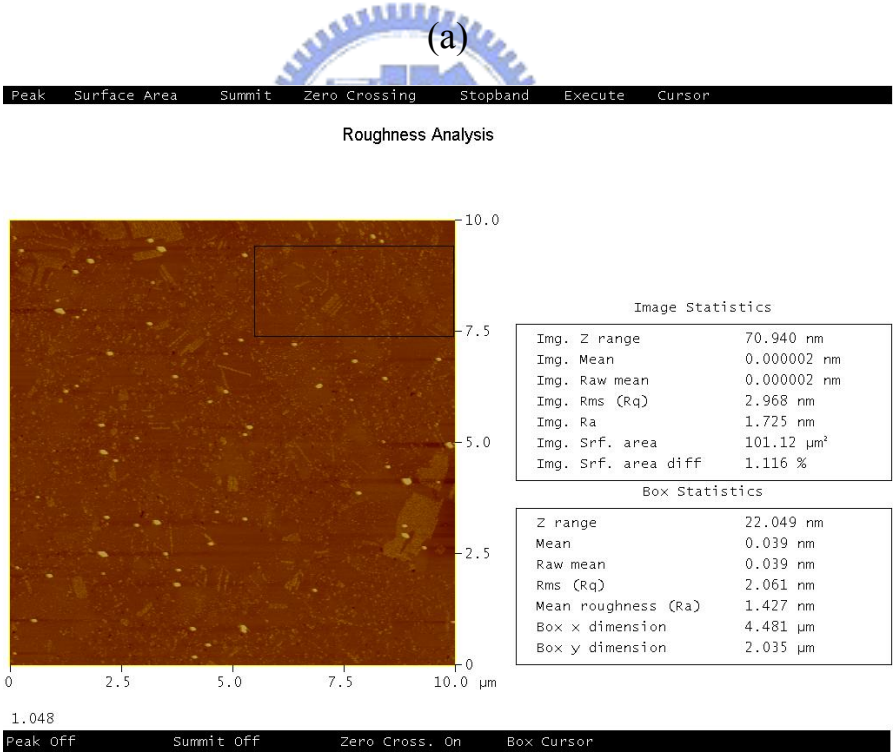

(b)

Figure.4-16 AFM images of polished copper film with HNO_3/PBTC-Na_4 =0.6/5E^{-3}M buffing, buffing time=1 min (a) 3D diagram (b)roughness analysis.

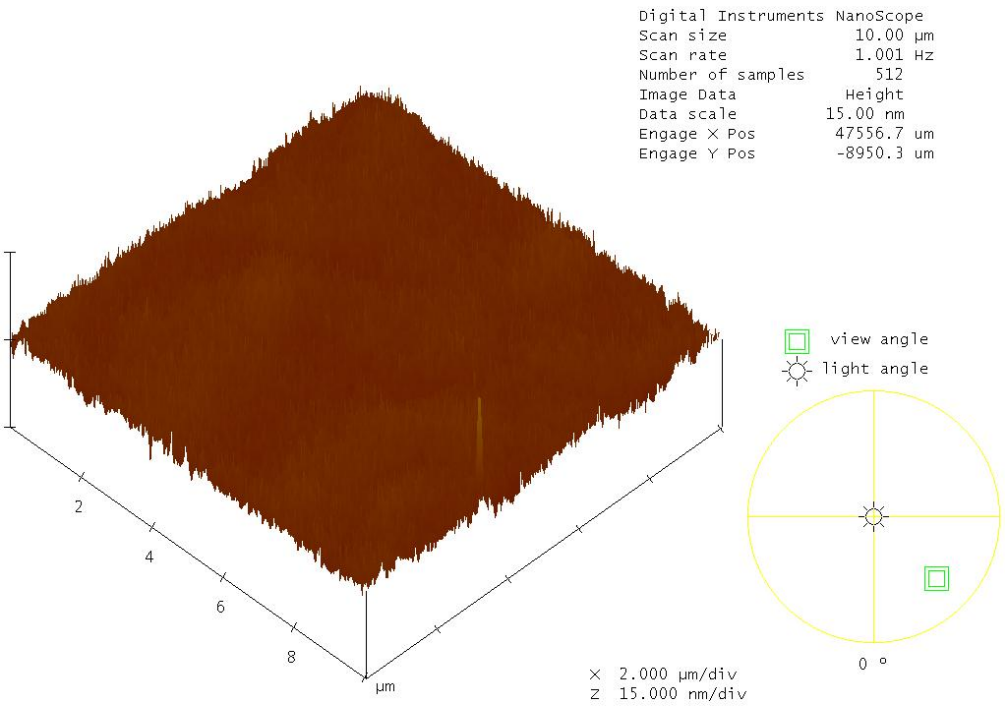

(a)

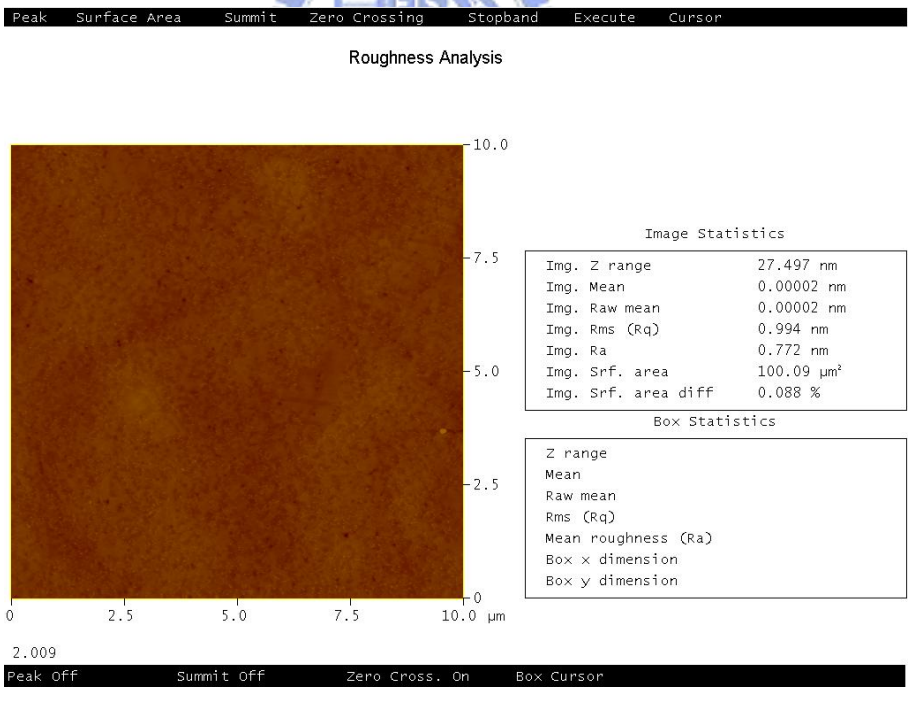

(b)

Figure.4-17 AFM images of polished copper film with HNO_3/ PBTC-Na_4 =0.6/5E^{-3}M buffing, buffing time=3 min (a) 3D diagram (b)roughness analysis.

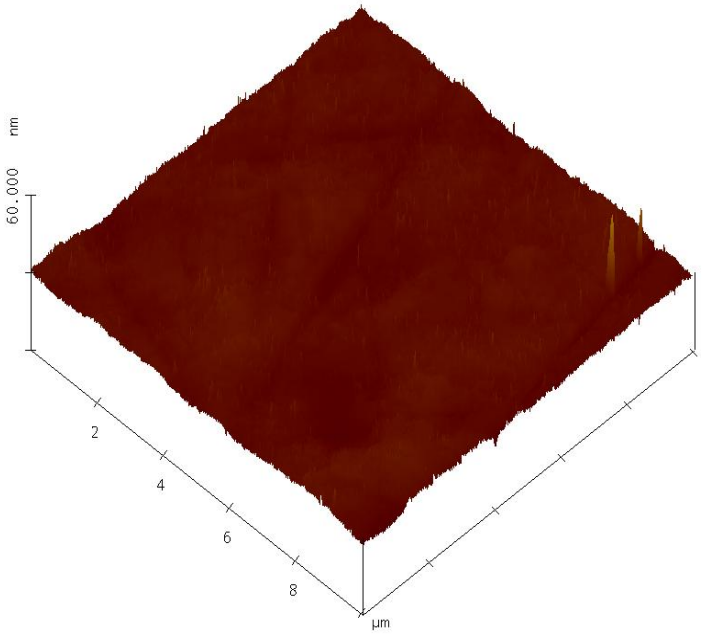

(a)

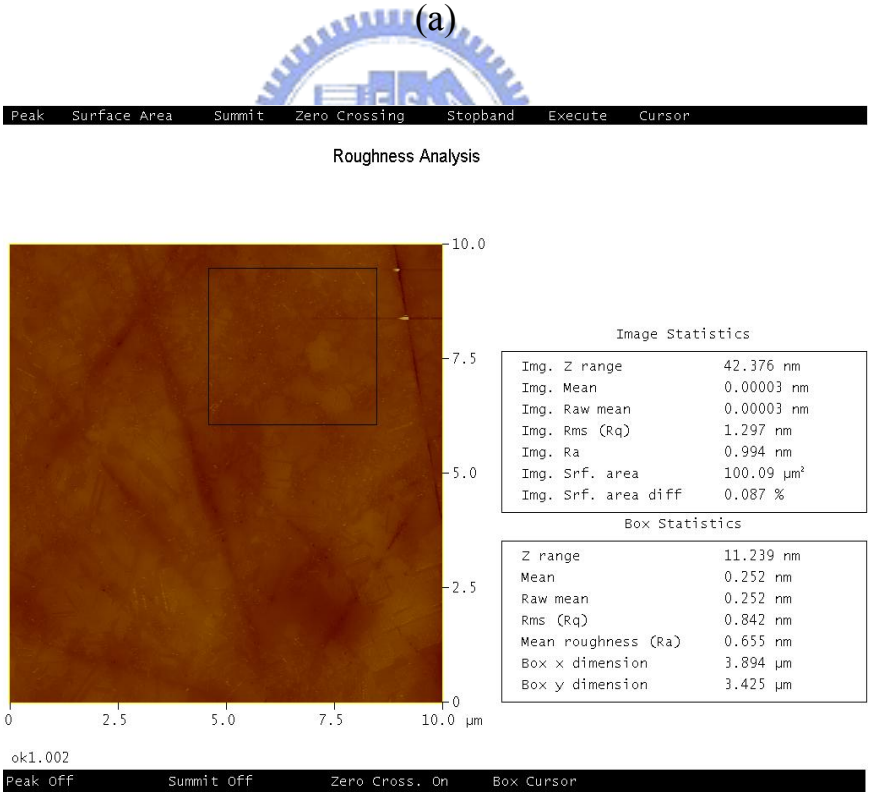

(b)

Figure.4-18 AFM images of polished copper film with HNO_3/PBTC-Na_4 =0.6/5E^{-3}M buffing, buffing time=6 min (a) 3D diagram (b)roughness analysis.

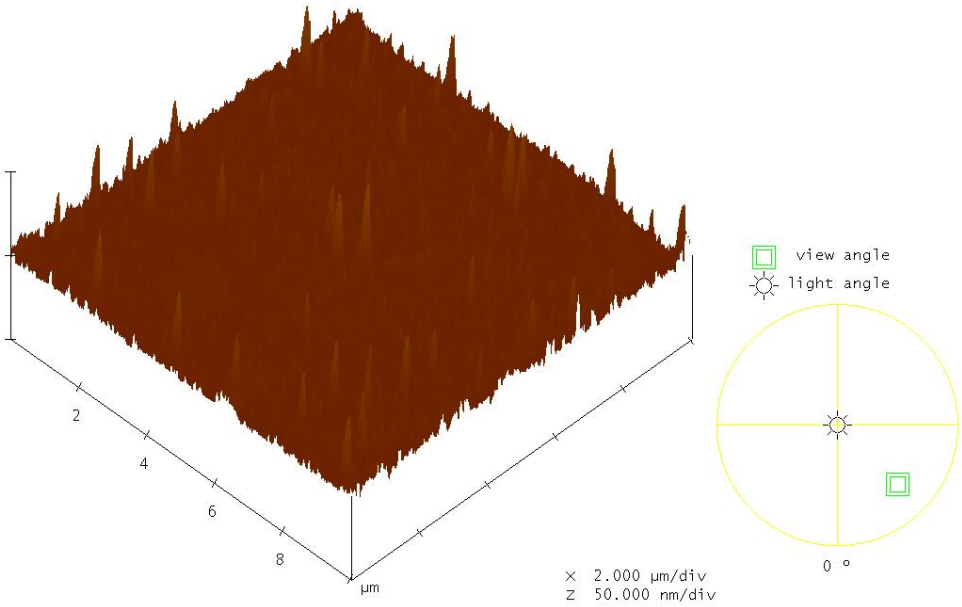

(a)

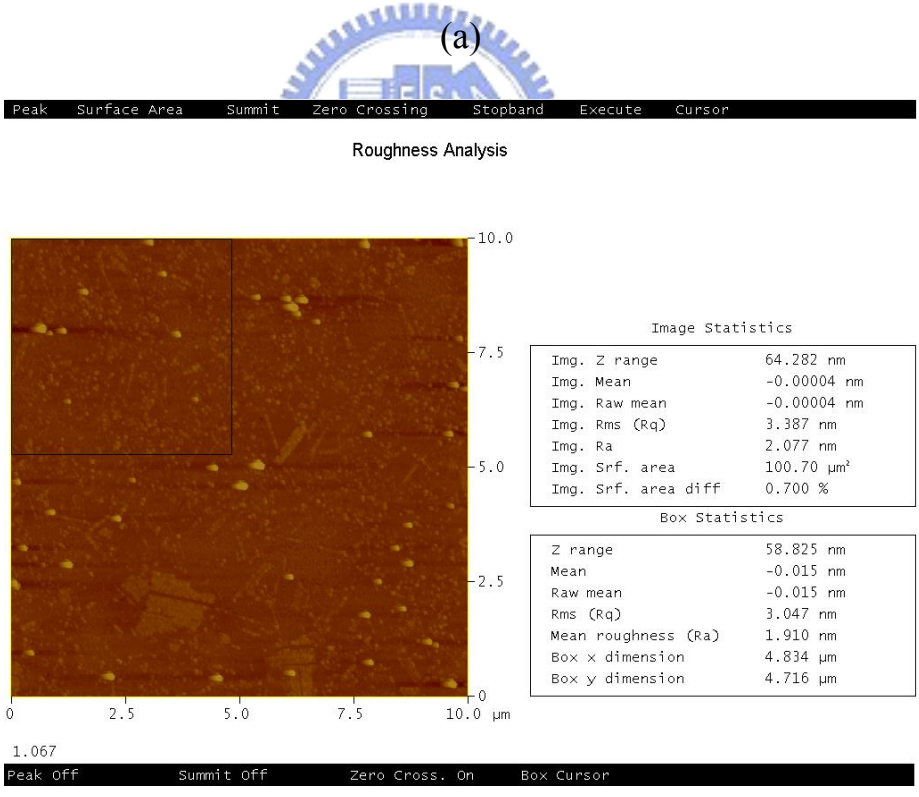

(b)

Figure.4-19 AFM images of polished copper film with HNO_3/ PBTC-Na_4 =0.6/1E^{-3}M buffing, buffing time=1min (a) 3D diagram (b)roughness analysis.

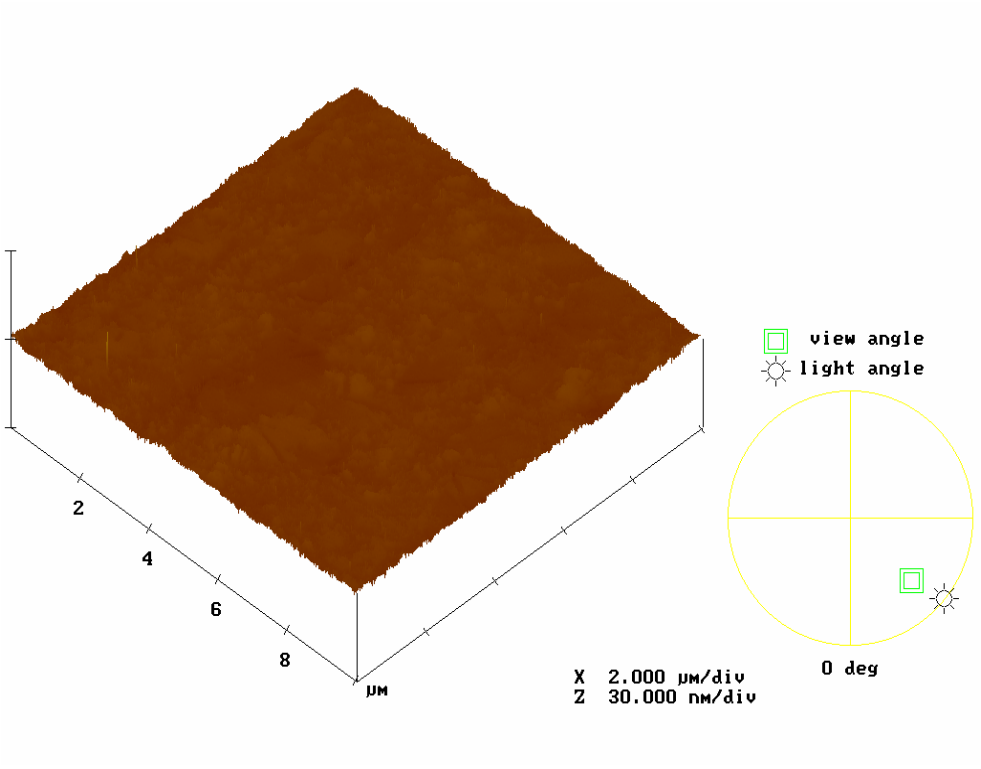

(a)

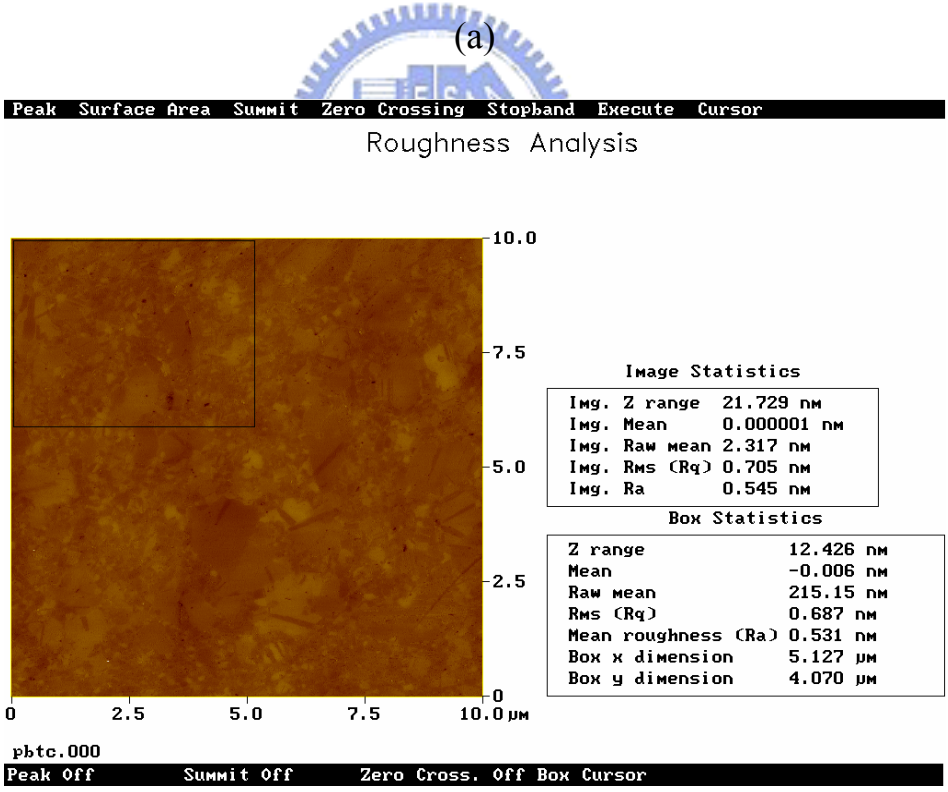

(b)

Figure.4-20 AFM images of polished copper film with HNO_3/ PBTC-Na_4 =0.6/1E^{-3}M buffing, buffing time=3min (a) 3D diagram (b)roughness analysis.

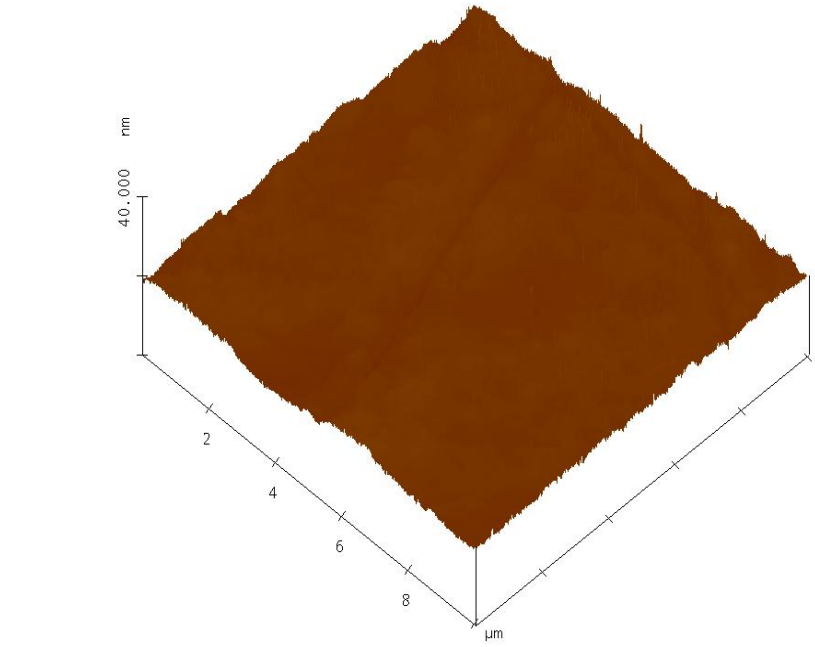

(a)

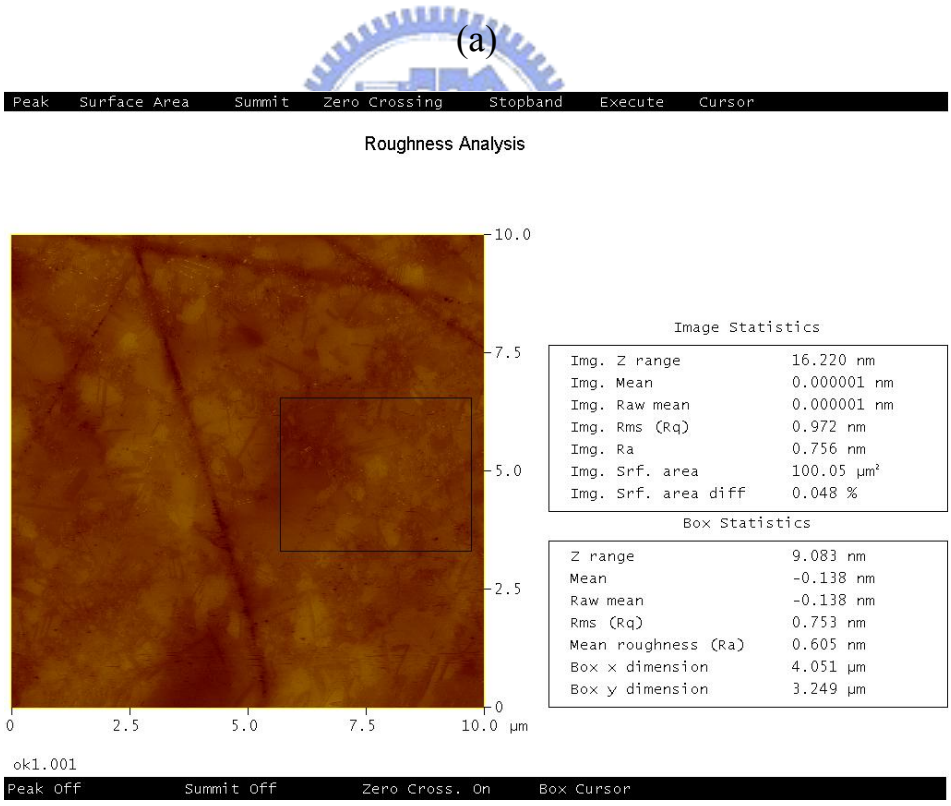

(b)

Figure.4-21 AFM images of polished copper film with HNO_3/ PBTC-Na_4 =0.6/1E^{-3}M buffing, buffing time=6 min (a) 3D diagram (b)roughness analysis.

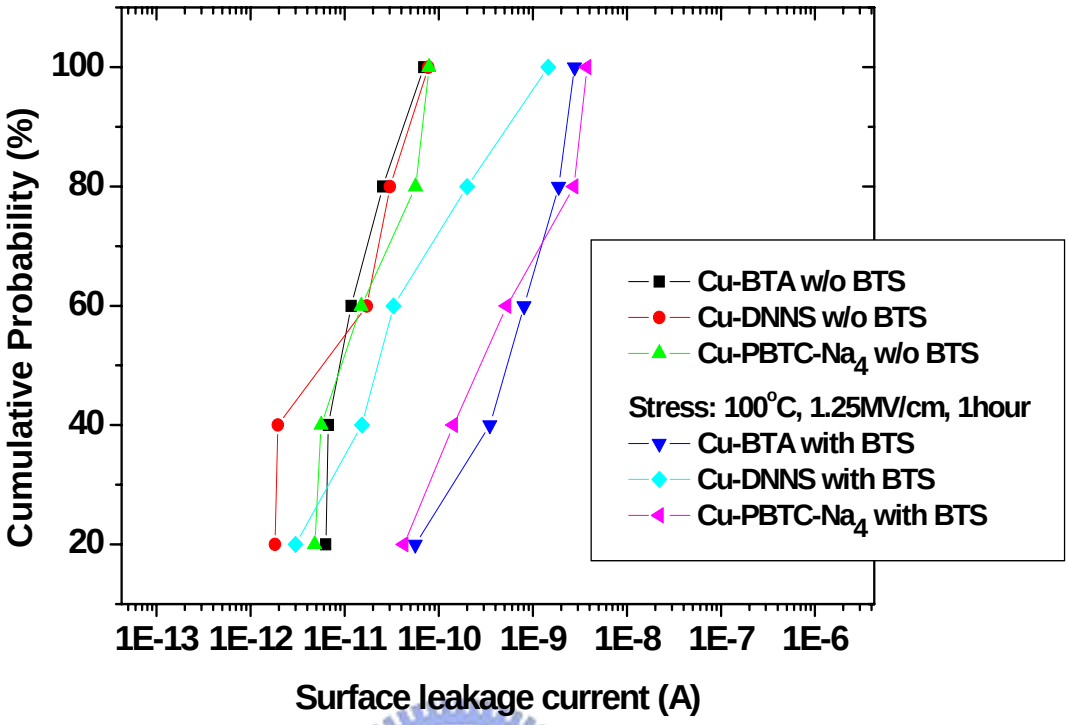

Figure.4-22 distribution of surface leakage current for Cu-comb interconnect measured at 90V

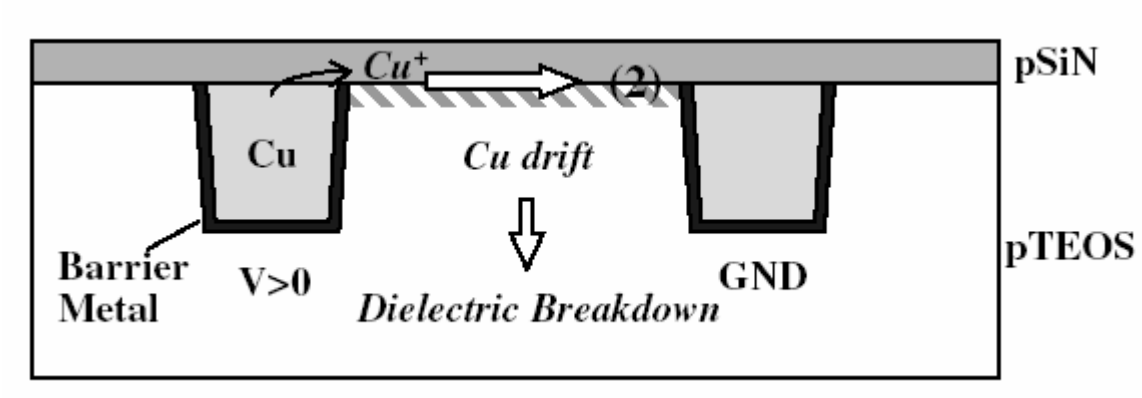

Figure.4-23 Dielectric degradation mechanism